Nisin-induced changes in *Bacillus* morphology suggest a paradigm of antibiotic action

Alexander J. Hyde, Judicaël Parisot, Adam McNichol, and Boyan B. Bonev*

School of Biomedical Sciences and Institute of Infection and Immunity, University of Nottingham, Nottingham NG7 2UH, United Kingdom

Edited by Jack L. Strominger, Harvard University, Cambridge, MA, and approved November 7, 2006 (received for review September 29, 2006)

Nisin is a small cationic lanthionine antibiotic produced by *Lactococcus lactis*. During its antimicrobial action, it targets intermediates in the bacterial cell-wall biosynthesis, lipid II, and undecaprenyl pyrophosphate. Here, we report results from electron microscopic investigations of the effects of lethal nisin doses on *Bacillus subtilis* cell morphology. Bacterial membranes were permeabilized shortly after *B. subtilis* was incubated with nisin, but this did not lead to immediate cell death. Cell division, as well as other life functions, persisted over at least half an hour after nisin was added. Slower bacterial elongation, consistent with cell envelope inhibition and accelerated division, resulted in cell-length reduction. Abnormal morphogenesis near the division site suggests this to be the primary site of nisin action. Morphological changes are characteristic of deregulation of a filamentous cell envelope protein, Mbl, and the division-inhibiting Min system. We propose a previously undescribed model, in which the lethal action of nisin against *B. subtilis* starts with membrane permeabilization and is followed by accelerated cell division, cell envelope inhibition, and aberrant cell morphogenesis.

cell wall | electron microscopy | bacterial morphology | lantibiotic | cell division

A widely used food preservative, the peptide antibiotic nisin, E234, (1, 2) is produced by *Lactococcus lactis* and shows high antimicrobial activity against a broad spectrum of Gram-positive bacteria. Nisin is also effective in inhibiting the outgrowth of spores from *Clostridium* and *Bacillus* species (3). Nisin activity toward Gram-negative organisms also has been reported, although to a lower degree than against Gram-positives and usually in combination with chelating agents (4, 5). Nisin is active in the nanomolar range and has no known toxicity to humans, which has placed it in the unique position of worldwide acceptance as a powerful and safe food additive in control of food spoilage (for a review, see ref. 6). The recent discoveries of lipid II as a target for nisin and, in particular, the pivotal role played by the pyrophosphate group, also have brought nisin to the forefront in the battle with resistant human infections as a model case for the design of new antibiotics.

The biosynthesis of nisin involves posttranslational modifications of ribosomally synthesized precursor peptide, which results in the formation of unusual amino acids (lanthionine, dehydroalanine, and dehydrobutyrine) (3, 7). Nisin is a positively charged peptide that is able to bind to negatively charged plasma membranes (8–11) via nonspecific electrostatic interactions. The antibacterial activity of nisin results from permeabilization of the cytoplasmic membrane and interference with the cell-wall biosynthesis of sensitive bacteria. During its action, nisin targets the cell wall precursors lipid II (12, 13) and undecaprenyl pyrophosphate (14).

Membrane permeabilization occurs after target recognition and nisin/lipid II complex formation (12). The process is rapid, with onset times ranging from milliseconds to seconds, and the lifetime of the pores can extend to seconds (13, 15). Pore formation leads to rapid dissipation of transmembrane electrostatic potential and vital solute gradients (4, 16, 17). The release of ATP, in particular, has been used to quantify nisin (18). Sahl and coworkers (19) demonstrated the importance of peptidoglycan inhibition during *in vivo* antimicrobial action of the lanthionine antibiotics gallidermin and epidermin.

Bacterial peptidoglycan is a dynamic system, in which biosynthetic incorporation of new peptidoglycan and degradation by autolysins are tightly coupled and controlled (20). The late stages of bacterial cell-wall biosynthesis take place on the outer leaflet of bacterial membrane, where biosynthesis intermediates are used as targets by a number cell wall-inhibiting antibiotics. In rod-shaped bacteria, peptidoglycan growth is most rapid during cell elongation and takes place, largely, near the division site (21, 22).

Cytokinesis in *B. subtilis* involves the protein *ftsZ*, which self-assembles into ring-shaped structures at mid-cell position, Z rings, at the beginning of the division process when the protein concentrations exceed 10 μM in the presence of GTP (23, 24). This process is normally suppressed by inhibitor protein systems, one of which is the Min system. In *Bacillus subtilis*, it consists of the *ftsZ* polymerisation inhibitor MinC and the protein MinD, an ATPase bound to the plasma membrane in its ATP-associated form and solublized upon nucleotide hydrolysis (25). In *B. subtilis* the Min proteins are tethered in to the bacterial poles by the protein DivIVA. Although the Min system does not determine the mid-cell localization of the division site, it serves to prevent polar division. Inactivation of the Min system may result in multiple septa formation (26, 27). When Z ring assembly is complete, cell-wall synthesis is switched from elongation to septal formation. Increased cellular concentrations of FtsZ lead to additional division events away from the normal midcell division sites and lead to the formation of minicells (28).

Cell shape determination in *B. subtilis* involves the protein Mbl, and deletion mutants show twisted and distorted phenotypes (29). The changes are more pronounced during rapid division, where *B. subtilis* cells often remain attached in chain-like structures (30). Errington and coworkers (30) report bulges and increased cellular width in the rapidly growing parts of *Bacillus* cells. Mbl also has been shown to affect the localization of FtsZ, a tubulin-like protein directing septal formation in prokaryotes. In normal cells, FtsZ self-associates approximately midway down the bacterial length to form closed division rings or Z rings, coaxial with the long axis of the rod. Instead, during division in Mbl mutants, FtsZ self-assembles into spirals in the mid-cell region of rapid growth (30). It has been suggested that helical Mbl filaments running underneath the plasma membrane are involved in anchoring the peptidoglycan and guide its formation along the cylindrical surface of the cell (31).

Here, we report results from electron microscopic investigation of short- and intermediate-term (5–10 min) changes in morphology of *B. subtilis* to lethal doses of nisin. We show the

Author contributions: A.J.H., J.P., and A.M. performed research; B.B.B. designed research; B.B.B. analyzed data; and B.B.B. wrote the paper.

The authors declare no conflict of interest.

This article is a PNAS direct submission.

*To whom correspondence should be addressed. E-mail: boyan.bonev@nottingham.ac.uk.

www.pnas.org/cgi/doi/10.1073/pnas.0608373104

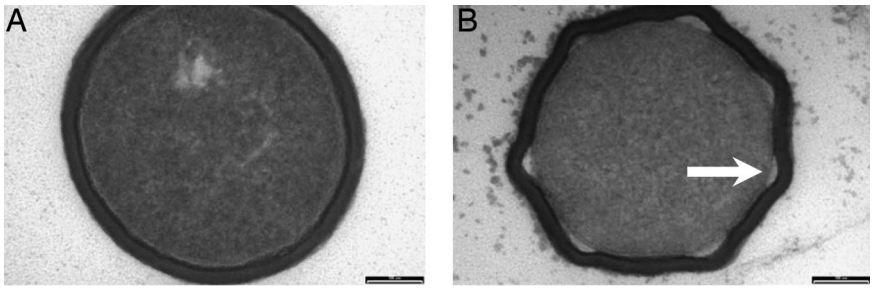

Fig. 1. Electron micrographs showing cross-sections of *B. subtilis* after mild hypotonic challenge. (*A*) No nisin. (*B*) After exposure to 5 μg/ml nisin. Detachment of the cell wall from the plasma membrane is clearly visible (arrow). (Scale bars: 100 nm.)

effects of rapid membrane permeabilization and subsequent length, cross-section, shape, and population distribution changes in bacilli. We outline the key changes taking place during cell-wall inhibition *in vivo*, which we believe lead to the ultimate decline in bacterial population. We proposed a model of nisin action, which relies on uncoupling of ATP-dependent pathways, regulating cell division, from the division process itself. We conclude that membrane permeabilization, followed by cell-wall inhibition and metabolic deregulation of bacterial division, is responsible for the lethal action of nisin against *B. subtilis*.

Results

The antimicrobial action of nisin is based on a combination of rapid events and longer timescale processes. Pore formation is a rapid process occurring over times on the order of milliseconds to seconds (15, 17, 32), whereas peptidoglycan inhibition has noticeable effects after periods on the order of hours (33). We have investigated the changes in morphology of *Bacillus* after *in vivo* exposure to nisin in liquid cultures both at the short and at the long time scales. Samples were collected 5 min after inoculation to observe immediate- and short-term effects of nisin *in vivo*, as well as at 20- and 30-min delays to investigate cell shape and population changes after short-term effects have subsided.

The addition of nisin to exponentially growing cells did not have an immediate effect at concentrations up to 50 μg/ml. However, 10 h after inoculation, bacterial density had declined in all samples with nisin concentrations >2.5 μg/ml, as determined by inhibition assays in liquid cultures.

Bacterial cultures were subjected to a mild osmotic challenge in 135 mM PBS and the membrane permeabilizing action of nisin was investigated at 15- and 30-min intervals after antibiotic addition. Electron micrographs in bacterial cross-section projections from untreated and nisin-treated cells are shown in Fig. 1. Cytoplasmic osmotic pressure aids adhesion of the plasma membrane to the peptidoglycan layer, which results in the circular cross-sections in untreated cells (Fig. 1*A*). Treatment with nisin at 5 μg/ml relieves the osmotic stress via pore formation and leads to the astral bacterial cross-sections seen in Fig. 1*B* after contraction of the plasma membrane. Partial cell-wall detachment from the plasma membrane is visible in Fig. 1*B*. This results from a decreased cytoplasmic volume after pore formation, which is not matched by a reduction in cell-wall length.

A better understanding of the differences between pore formation and cell-wall inhibition can be obtained by analyzing the cell-wall length in the cross-section and comparing it to the bacterial diameter, measured within the plasma membrane. Fig. 2*A* shows the average cell-wall length of untreated bacteria and bacteria exposed to nisin at 5, 10, 20, and 30 μg/ml. We observed no statistically significant variation between untreated and nisin-treated samples, which indicates that cell-wall degradation along the circumference is insignificant on this time scale. In contrast, the average bacterial cross-section was noticeably reduced from $\approx$0.58–0.59 μm to 0.44–0.48 μm after the addition of nisin, which is consistent with the occurrence of nisin-induced pores during the period of osmotic challenge (Fig. 2*B*). There was statistically significant dependence of cell diameter on nisin concentration.

We used electron microscopy to investigate the effects of nisin on bacterial length and division. Histograms of bacterial lengths

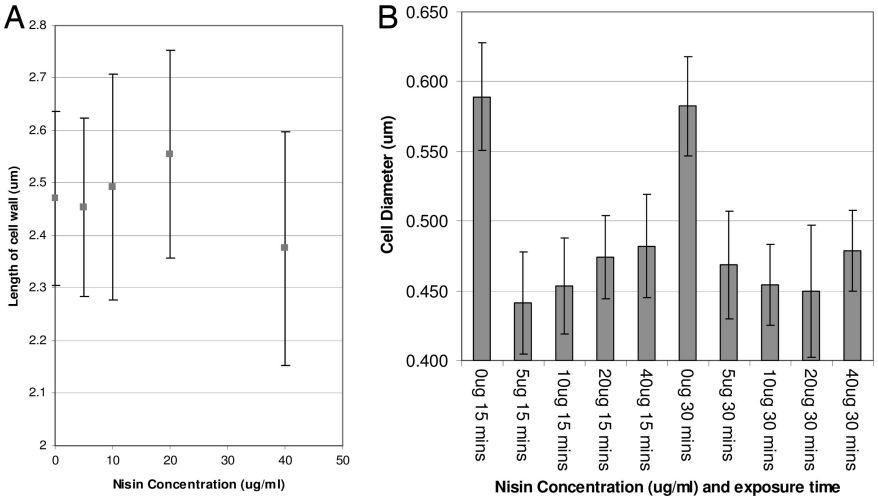

Fig. 2. Total length of *B. subtilis* cell wall in transverse bacterial cross-section (*A*) and cell diameter at the plasma membrane after a mild hypotonic challenge (*B*). Luminal cross-section is reduced without concomitant reduction in cell-wall length.

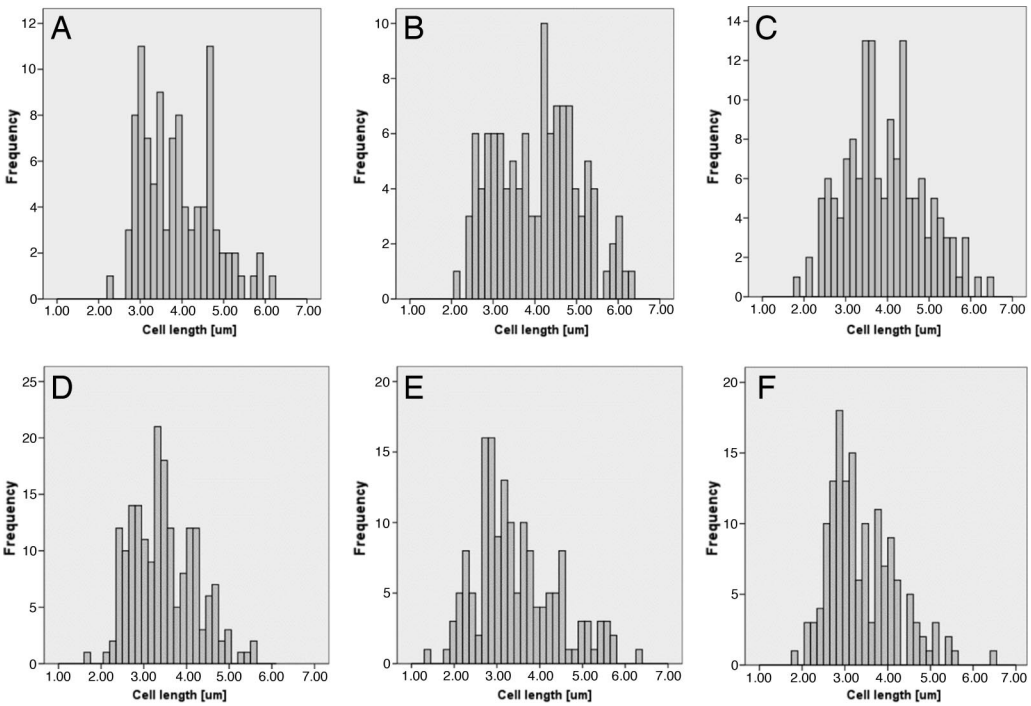

Fig. 3. Histogram of *B. subtilis* cell length at 5 (*A* and *D*), 20 (*B* and *E*), and 30 (*C* and *F*) min after incubation with nisin. (*A–C*) Control. (*D–F*) After treatment with 5 μg/ml nisin.

are shown in Fig. 3. Contributions from different periods in the cell cycle determine the shape of the distribution (Fig. 3*A*). Cell lengths of $\approx$3.5 μm can be attributed to the interphase and contribute to the lower length region. Elongating and dividing populations show high frequency at lengths of 4.5 μm and reach lengths as high as 5.5 μm.

Samples for electron microscopy were collected at times 5, 20, and 30 min after the addition of nisin at 5 μg/ml. Histograms of bacterial cell lengths are shown in Fig. 3 *D*, *E*, and *F*, respectively, with control samples lacking nisin in Fig. 3 *A*, *B*, and *C*. The average interphase cell length 5 min after inoculation remained at $\approx$3.5 μm. However, the dividing population appeared reduced. Because we did not observe an increase in bacterial ghost counts, we concluded that nisin had stimulated cell division, rather than killing longer cells. The average bacterial length of the entire bacterial population decreased from 3.9 μm in the untreated samples to 3.5 μm after treatment with 5 μg/ml nisin (Table 1).

After 20- and 30-min delays after nisin incubation, we observed a reduction in the average bacterial cell length from 3.9 to $\approx$3.4 μm (Fig. 3 *E* and *F*). The distribution is skewed toward lower bacterial lengths 30 min after nisin addition, whereas bacterial division continues. The approximate length of the dividing population was lower than the observed 4.5 μm in the control sample.

Table 1. Average pole to pole and pole to septum length, *l*, standard deviation of distributions, Δl, and total population per sample from untreated *B. subtilis* cells and cells treated with nisin and decoynine

	5 min		20 min		30 min	
Nisin	No nisin	5 μg/ml	No nisin	5 μg/ml	No nisin	5 μg/ml
l, μm	3.9	3.5	4.1	3.4	3.9	3.4
Δl, μm	0.84	0.75	1.00	0.96	0.94	0.80
Counts	102	187	118	156	150	150

To obtain further insight into the effects of nisin on bacterial cell division and the role of GTP, we treated *B. subtilis* cultures with a lethal concentration of 50 μg/ml nisin (Fig. 4*C*) and with the GTPase inhibitor decoynine (Fig. 4*D*). Decoynine treatment leads to GTP but not ATP depletion (34) and does not reduce FtsZ levels in *L. lactis* (35). The bacterial population remained viable 30 min after treatment in both cases. The nisin-treated cultures showed significant reduction in the average cell length from 3.9 μm to $\approx$2.5 μm. Incubation with decoynine led to a notable reduction in the average cell length to 3.1 μm with a broad dispersion of cell lengths showing no distinct interphase or division regions.

We analyzed the shape of the bacterial length distributions to investigate any effects of nisin on the relative population in different phases of bacterial life cycle. We used skewness and kurtosis to compare the observed bacterial length distributions to a normal distribution. Error-corrected skewness/error and kurtosis/error data from samples treated with 5 μg/ml nisin and from untreated controls at 5, 20, and 30 min after nisin-treatment are summarized in Table 2. No significant deviation form symmetry or from normal distribution was observed in the control samples. Five minutes after treatment with 5 μg/ml nisin, we did not observe significant changes in the distribution profile. At later times, 20 and 30 min after treatment, skewness values of 3.5 and 4.7 revealed a shift in the population toward shorter, interphase cell lengths. Within the experimental error, kurtosis analysis revealed no significant deviation from a normal distribution.

Values of error-corrected skewness and curtosis from samples treated with 0, 5, and 50 μg/ml nisin and with the GTPase inhibitor decoynine 30 min after the addition of each compound are shown in Table 3. A departure from symmetry is seen in the change in skewness from 1.4 in the untreated case to 4.7 in the presence of 5 μg/ml nisin and to 9.1 at a nisin concentration of 50 μg/ml. This indicates higher frequencies at shorter wave-

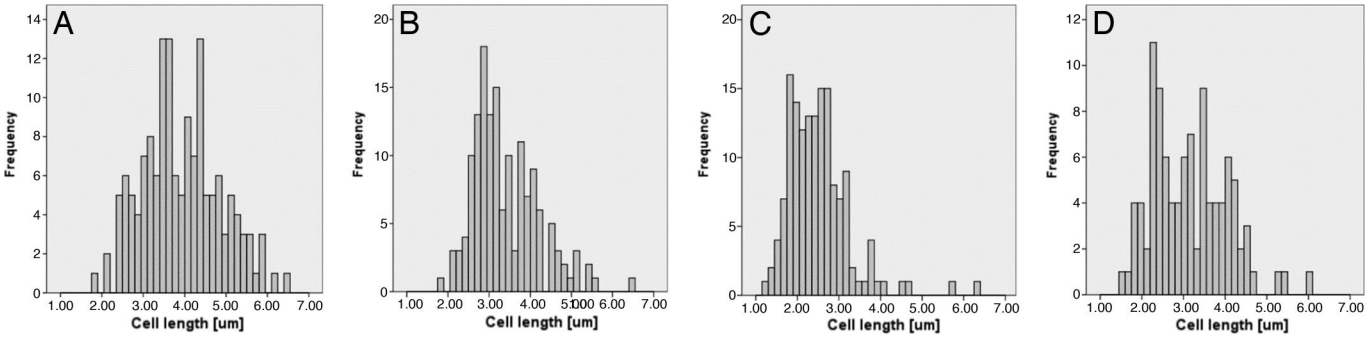

Fig. 4. Histogram of *B. subtilis* cell length 30 min after exposure to 5 and 50 μg/ml nisin. (*A*) Control. (*B*) After exposure to 5 μg/ml nisin. (*C*) After exposure to 50 μg/ml nisin. (*D*) After treatment with GTPase inhibitor decoynine. Dose-dependent decrease in cell length is evident.

lengths, consistent with shortening of the bacterial population and a preferential population of the interphase. The value of kurtosis also increased from –1.08 in untreated samples, well with the normal range, to 15.4 after incubation with 50 μg/ml nisin. This is consistent with a focused short-length distribution and a "tail" of longer bacteria.

Although addition of decoynine lead to a reduction in the average bacterial length from 3.9 μm to 3.1 μm, the population distribution remained the same as in the untreated case. Skewness revealed a symmetric distribution and kurtosis remained within the range indicative of a normal distribution, suggesting no departure from the normal cell cycle population.

Fig. 5*A* shows the normal progression of septal formation in *B. subtilis*. By contrast, the addition of 5 μg/ml nisin resulted in multiseptal divisions, often showing two closely located septa (Fig. 5*B*). This is consistent with a model in which ATP deregulation during pore formation by nisin may stimulate spontaneous septation and uncontrolled cell division. Similar formation of multiple septa close to the mid-cell site in *B. subtilis* has been observed in cells in which the division-suppressing Min system has been suppressed (26).

When the concentration of nisin is increased 10-fold to 50 μg/ml, not only is the septation control disrupted but the formation of septa during division also can be affected. Cell-wall inhibition in the region of rapid growth near the septation site can lead to a reduction in cell length and aberrant morphogenesis. Fig. 5 shows examples of morphological aberrations during septation. These include multiple septation (Fig. 5*C*), disjointed helical septa (Fig. 5*D*), "corkscrew" cell-wall morphologies (Fig. 5*E*), and septal malformation (Fig. 5*F*). One example of division "dead end" is the reduction of bacteria to large numbers of nonviable "minicells," devoid of a complete DNA set (Fig. 5*G*). The formation of minicells has been reported when the cellular concentration of FtsZ has been raised (28). Long, aseptal cells also were observed after exposure to high nisin concentrations.

Discussion

In the present study, we investigate the morphological changes in *B. subtilis*, a Gram-positive rod, after incubation with nisin to analyze the effects of the antibiotic during its bactericidal action *in vivo*. We observed morphological changes consistent with both membrane poration and cell-wall inhibition. Our results show that pore formation by treatment with nisin at a concentration exceeding the minimal inhibitory concentration does not have an immediate bactericidal effect but has longer-term consequences, and cell demise results mainly from metabolic deregulation and cell growth inhibition. We also were able to show that the most severe cell-wall malformation occurs in the region of rapid cell-wall growth near the site of septal formation, which highlights this region as the principal site of action for nisin.

To examine the consequences of membrane permeabilization by nisin and the role osmotic pressure plays in maintaining cell shape, we introduced untreated and nisin-treated *B. subtilis* cells into a hypotonic environment. Plasma membrane integrity was maintained in untreated cells, and the membrane adhered well to the cell wall, which was drawn to its maximum cross-area shape, a circle, by the osmotic pressure of its cytoplasmic constituents. By contrast, nisin-treated cells showed a reduced cytoplasmic cross-section, which indicates efflux of cytoplasmic constituents. In the short-term (5 min after exposure), cell-wall thickness remained unchanged, which emphasized the different time scales of pore formation and cell-wall inhibition.

The osmotic stress collapse also led to partial detachment of the plasma membrane from the cell wall. One possible explanation may be sought in considering the surfactant properties of nisin molecules, which may be capable of intercalating between pyrophosphate-linked cell-wall anchors and the plasma membrane. This would withdraw partially the isoprenyl anchor chains from the membrane and weaken cell-wall adhesion. Another manifestation of the reduced membrane adhesion to the peptidoglycan can be seen in Fig. 5*F*, where septal peptidoglycan growth is seen away from the membrane into the cytoplasmic space.

The most significant effects of nisin on *B. subtilis* were seen at later times of 20 and 30 min after exposure. The overall pole-to-pole and pole-to-septum average cell length decreased in comparison with the untreated cells. This demonstrates the cell-wall inhibitory action of nisin, which has been predicted from its interactions with lipid II and undecaprenyl pyrophosphate and observed in chemically modified nisin (13, 14, 32). One important point is that the reduction in cell length from $\approx$4.0 μm in untreated samples to 3.5 μm in the presence of 5

Table 2. Skewness/error and kurtosis/error values from cell length distribution of *B. subtilis* cells treated with 5 μg/ml nisin

	5 min		20 min		30 min	
Nisin	No nisin	5 μg/ml	No nisin	5 μg/ml	No nisin	5 μg/ml
Skewness	2.3	2.5	0.64	3.5	1.4	4.7
Kurtosis	−0.66	−0.42	−1.84	0.20	−1.08	2.56

Table 3. Skewness/error and kurtosis/error values from cell-length distribution of *B. subtilis* cells 30 min after treatment with 5 and 50 μg/ml nisin and decoynine at 500 μg/ml

Nisin	No nisin	5 μg/ml	50 μg/ml	Decoynine
Skewness	1.40	4.69	9.13	2.19
Kurtosis	−1.08	2.56	15.4	0.09

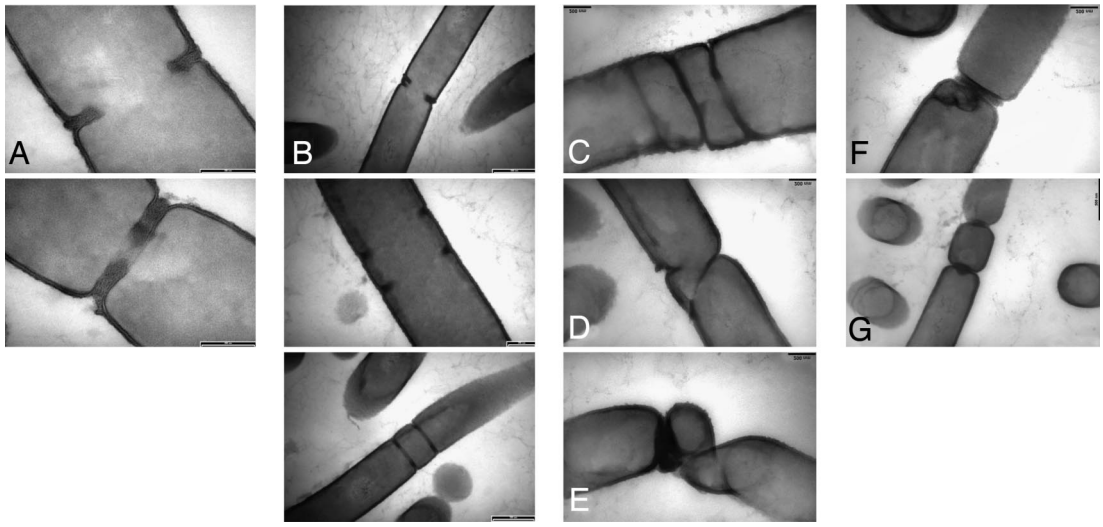

Fig. 5. Electron micrographs showing morphogenesis during cell division. (*A*) Septal formation in untreated *B. subtilis*. (*B*) Multiple septation 30 min after treatment with 5 μg/ml nisin. (*C–F*) Aberrant morphogenesis after treatment with 50 μg/ml nisin. (*G*) The formation of minicells. (*C–F*) Multiple septation with abnormal septal orientation and cell swelling (*C*), helical septal formation (*D*), corkscrew growth of the cell envelope in the growth region near the division site (*E*), and septal malformation and cell-wall formation away from the cell surface (*F*). (Scale bars: 200 nm, except *B Top* and *Bottom* and *F*, 500 nm.)

μg/ml nisin was achieved within the first 5 min after treatment. This is surprising, because the duplication times in *B. subtilis* are in the order of 30 min. Distribution analysis 30 minutes after the addition of nisin revealed a relative increase in frequencies of short bacteria, which suggests that more cells have progressed through division into the interphase than in the control sample. These observations suggest that nisin does not inhibit cell division but, to the contrary, appears to drive the population through division and to synchronize the bacterial development through the cell cycle, in the short term at least.

The morphological changes after cell-wall inhibition by nisin are rather different from those observed after treatment with penicillin or vancomycin, which reflects the differences in mode and site of action between these antibiotics. We did not observe blebbing, spheroplasts, or the formation of a filamentous cell wall as seen in *Staphylococcus aureus* after penicillin treatment (36), and we did not see cell wall thinning, as seen after vancomycin treatment. The reduction in cell length, which we observed instead, indicates that cell-wall inhibition occurs mainly during the active cell elongation of bacteria division cycle. We also observed an increase in bacterial diameter in the immediate vicinity of the newly forming septa, which reinforces the conclusion that nisin inhibits cell-wall formation predominantly on the newly formed cell wall near the septation site. While this work was under review, a report (37) appeared that describes a mechanism of action for lanthionine antibiotics by means of pyrophosphate-mediated sequestering of lipid II from sites of bacterial cell-wall generation. These results are in agreement with our findings of significant aberrations in cell-wall morphogenesis, where bacterial elongation is rapid.

In our studies, the samples treated with nisin revealed a high frequency of double septa forming near one another and a number of multiseptal bacteria, where up to four septa appeared in the midcell division region (Fig. 5*C*). One possible explanation is that ATP-dependent septation-repressor mechanisms, such as the Min system (38), are deregulated after membrane permeabilization, whereas septal formation continues. Because the action of nisin leads to efflux of ATP (17), the spatial regulation of Z ring formation is likely to be affected and favorable conditions for Z ring formation can occur over a division "band," rather than a specific site. At the same time, reduction in cytoplasmic GTP levels may be insufficient to prevent FtsZ self-association, which has been reported to continue at GTP concentrations only one-10th of their normal value (39).

In *B. subtilis*, Mbl has been shown to localize in helical filaments, running along the length of the cell (30). Mbl deletion mutants show characteristic shape deformations, namely twisted phenotypes with increased cell diameter and other deformations, that are particularly well pronounced near the mid-cell division region. In our study, we observed similar helical formation of the septa after exposure to high doses of nisin (Fig. 5*D*) and cell widening in the region of axial growth near the division site (Fig. 5*F*) and helical cell-wall morphogenesis.

Minicell formation has been observed in the presence of elevated FtsZ concentrations (28). We observed a large number of minicells after exposure of *B. subtilis* to high doses of nisin. These minicells appeared around the midcell septal doubling site, observed after treatment with lower nisin doses. As septal completion appears accelerated at higher nisin doses, minicells are most likely the end result of complete multiseptal formation.

Conclusions

Nisin induced leakage of cytoplasmic contents from treated samples, which we saw as a reduction of bacterial cross-section. Septal formation continued in the presence of nisin, although it displayed multiple aberrations. Cytokinesis was evident 30 min after addition of nisin, which contradicts the current view of a rapid cell death after antibiotic addition. The principal site of cell-wall inhibition by nisin appears near the division site, where peptidoglycan formation is accelerated. We propose a picture of nisin action, in which nisin permeabilizes plasma membranes, accelerates cell division and causes minicell formation. Nisin also deregulates cell envelope formation, which leads to aberrant cell morphogenesis. The proposed mechanism is distinctly different from cell-wall inhibition by glycopeptide and β-lactam antibiotics and the action of other pore-forming peptides.

Materials and Methods

Bacterial Strains. Plasmid-free nisin-producing strain *Lactococcus lactis* FI5876, *L. lactis* MG1614, lacking the nisin production gene and subtilin-producing *B. subtilis* ATCC 6633 were a kind gift from Hikki Horn, Arjan Narbad, and Mike Gasson (Biotechnology and Biological Sciences Research Council Institute for Food Research, Norwich, U.K.). Nisin was produced from *L.*

lactis FI5876 and purified by hydrophobic chromatography and reverse-phase HPLC as described in ref. 40. Inhibitory activity of nisin was tested by disk diffusion in agar (41, 42) and in liquid medium against *L. lactis* MG1614. *B. subtilis* ATCC 6633 was grown in Luria broth at 37°C to $OD_{600} = 1.0$. Nisin then was added to 50-μl culture aliquots at concentrations of 0, 5, 10, 20, 40, and 50 μg/ml, and the culture was incubated for an additional 15 or 30 min at 37°C. Care was taken to maintain comparable bacterial counts in all experiments because nisin partitions preferentially onto the polar/apolar interfaces of membranes, which can lead to significant variation in therapeutic surface densities of the antibiotic. Decoynine was added at 500 μg/ml, and cells were harvested after 30 min of incubation at 37°C.

Electron Microscopy. Bacterial pellets were washed with 50 mM phosphate buffer (pH 6.9) and centrifuged at 3,000 $\times$ *g* for 15 min. Cells were fixed in 3% glutaraldehyde in 0.1 M cacodylate buffer (pH 7.2) overnight. Pellets were postfixed in 1% aqueous osmium tetroxide for 30 min and set in 4% agarose. They were dehydrated in a graded ethanol series and embedded in Transmit low viscosity resin (TAAB). Ultrathin sections (70–90 nm) were cut by using a Reichert-Jung Ultracut E ultramicrotome (Leica, Milton Keynes, U.K.) and collected on 100 hex copper grids. They were contrasted by using uranyl acetate and lead citrate and viewed by using a 1010 TEM (JEOL, Welwyn Garden City, U.K.) operated at 80 kV with digital image acquisition. Measurements of overall cell length, cell diameter, and cell-wall length were taken by using Openlab 4.0.1 software (Improvision, Coventry, U.K.).

Statistical Analysis of Cell Lengths. Statistical analysis was performed by using SPSS. We used skewness and kurtosis to describe the deviation of all length distributions from normal.

Skewness and kurtosis relate to the third and fourth distribution moments, adapted to discrete variables. We have used the ratios of skewness and kurtosis to their associated errors. Values falling within the range ± 2 indicate no departure from symmetric and normal distributions, respectively.

We thank Nikki Horn, Arjan Narbad, and Mike Gasson for the gift of *Lactococcus* and *Bacillus* strains and Terry Mayhew for his useful comments and suggestions. We acknowledge the financial support of Biotechnology and Biological Sciences Research Council of the U.K. Grant B20039 (to B.B.B.)

1. Rogers LA, Whittier EO (1928) *J Bacteriol* 16:211–229.
2. Delves-Broughton J, Blackburn P, Evans RJ, Hugenholtz J (1996) *Int J Gen Mol Microbiol* 69:193–202.
3. Rayman MK, Aris B, Hurst A (1981) *Appl Environ Microbiol* 41:375–380.
4. Abee T, Rombouts FM, Hugenholtz J, Guihard G, Letellier L (1994) *Appl Environ Microbiol* 60:1962–1968.
5. Delves-Broughton J (1990) *Food Technol* 44:100–117.
6. Thomas LV, Clarkson MR, Delves-Broughton J (2000) in *Natural Food Antimicrobial Systems*, ed Naidu AS (CRC, New York) pp 463–524.
7. Gross E, Morell JL (1971) *J Am Chem Soc* 93:4634–4635.
8. Bonev BB, Chan WC, Bycroft BW, Roberts GCK, Watts A (2000) *Biochemistry* 39:11425–11433.
9. Breukink E, Ganz P, de Kruijff B, Seelig J (2000) *Biochemistry* 39:10247–10254.
10. Breukink E, vanKraaij C, Demel RA, Siezen RJ, Kuipers OP, de Kruijff B (1997) *Biochemistry* 3:6968–6976.
11. Liu W, Hansen JN (1990) *Appl Environ Microbiol* 56:2551–2558.
12. Breukink E, Wiedemann I, van Kraaij C, Kuipers OP, Sahl H-G, de Kruijff B (1999) *Science* 286:2361–2364.
13. Wiedemann I, Breukink E, van Kraaij C, Kuipers OP, Bierbaum G, de Kruijff B, Sahl H-G (2001) *J Biol Chem* 276:1772–1779.
14. Bonev BB, Breukink E, Swiezewska E, de Kruijff B, Watts A (2004) *FASEB J* 18:1862–1869.
15. Ruhr E, Sahl H-G (1985) *Antimicrob Agents Chemother* 27:841–845.
16. Chan WC, Leyland M, Clark J, Dodd HM, Lian LY, Gasson MJ, Bycroft BW, Roberts GCK (1996) *FEBS Lett* 390:129–132.
17. Sahl H-G (1991) *Nisin and Novel Lantibiotics*, eds Jung G, Sahl H-G (ESCOM, Leiden, The Netherlands) pp 347–358.
18. Waites MJ, Ogden K (1987) *J Inst Brew* 93:30–32.
19. Bonelli RR, Schneider T, Sahl H-G, Wiedemann I (2006) *Antimicrob Agents Chemother* 50:1449–1457.
20. Höltje JV (1998) *Microbiol Mol Biol Rev* 62:181–203.
21. Daniel RA, Errington J (2003) *Cell* 113:767–776.
22. Tiyanont K, Doan T, Lazarus MB, Fang X, Rudner DZ, Walker S (2006) *Proc Natl Acad Sci USA* 103:11033–11038.
23. Autret S, Errington J (2001) *Dev Cell* 1:10–11.
24. Mukherjee A, Dai K, Lutkenhaus J (1993) *Proc Natl Acad Sci USA* 90:1053–1057.
25. Margolin W (2005) *Nat Rev Mol Cell Biol* 6:862–871.
26. Anderson DE, Gueiros-Filho FJ, Erickson HP (2004) *J Bacteriol* 186:5775–5781.
27. Sun Q, Margolin W (2004) *J Bacteriol* 186:3951–3959.
28. Ward JE, Lutkenhaus J (1985) *Cell* 42:941–949.
29. Abhayawardhane Y, Stewart GC (1995) *J Bacteriol* 177:765–773.
30. Jones LJF, Carballido-Lopez R, Errington J (2001) *Cell* 104:913–922.
31. Leaver M, Errington J (2005) *Mol Microbiol* 57:1196–1209.
32. Breukink E, de Kruijff B (1999) *Biochim Biophys Acta* 1462:223–234.
33. Ayusawa D, Yoneda Y, Yamane K, Maruo B (1975) *J Bacteriol* 124:459–469.
34. Mitani T, Heinze JE, Freese E (1977) *Bioch Biophys Res Comm* 77:1118–1126.
35. Beyer NH, Roepstorff P, Hammer K, Kilstrup M (2003) *Proteomics* 3:786–797.
36. Scholar EM, Pratt WB (2000) *The Antimicrobial Drugs* (Oxford Univ Press, New York), 2nd Ed.
37. Hasper HE, Kramer NE, Smith JL, Hillman JD, Zachariah C, Kuipers OP, de Kruijff B, Breukink E (2006) *Science* 313:1636–1637.
38. Hu ZL, Saez C, Lutkenhaus J (2003) *J Bacteriol* 185:196–203.
39. Chen YD, Erickson HP (2005) *J Biol Chem* 280:22549–22554.
40. de Vos WM, Mulders JWM, Siezen RJ, Hugenholtz J, Kuipers OP (1993) *Appl Environ Microbiol* 59:213–218.
41. Cooper KE (1955) *Nature* 176:510–511.
42. Finn RK (1959) *Anal Chem* 31:975–977.